Heterogeneous responses to embryonic critical period perturbations among different components of the *Drosophila* larval locomotor circuit.

Niklas Krick*[1], Jacob Davies*[2], Bramwell Coulson*[2], Daniel Sobrido-Cameán[1], Michael Miller[1], Matthew C. W. Oswald[1], Aref A. Zarin[3], Richard Baines[#2], Matthias Landgraf[#1]

* = joint first authors

= joint senior and corresponding authors

Affiliations:

1 Department of Zoology, University of Cambridge, Cambridge CB2 3EJ, United Kingdom

2 Division of Neuroscience and Experimental Psychology, School of Biological Sciences, Faculty of Biology, Medicine and Health, University of Manchester, Manchester M13 9PT, United Kingdom

3 Department of Biology, Texas A&M University, College Station, Texas 77843-3258

Abstract

As developing neural circuits become functional, they undergo a phase of heightened plasticity in response to intrinsic and/or extrinsic stimuli. These developmental windows are termed critical periods (CPs), because perturbations during the CP can lead to lasting and significant change in subsequent development, such as sub-optimal and/or unstable networks. By contrast, the same manipulations before or after the CP does not create lasting changes. Here, we have used the *Drosophila* larval locomotor network to study how different identified, connected elements respond to a CP perturbation, from pre-motor interneuron to motoneuron, to neuromuscular junction. Using heat stress as an ecologically relevant stimulus, we show that increasing temperature causes increased network activity that, when applied during the CP, leads to larvae that crawl more slowly and that require longer to recover from electroshock-

induced seizures, indicative of decreased network stability. Within the central nervous system, we find CP perturbation leads to pre-motor interneurons delivering increased synaptic drive to motoneurons, which in turn display reduced excitability. The peripheral neuromuscular junction, on the other hand, maintains normal synaptic transmission, despite significant structural changes of synaptic terminal overgrowth and altered postsynaptic receptor field composition. Overall, our data demonstrate that different connected elements within a network respond differentially to a CP perturbation. Our results suggest an underlying sequence, or hierarchy, of network adjustment during developmental CPs, and present the larval locomotor network as a highly tractable experimental model system with which to study CP biology.

Introduction

During nervous system development, critical periods (CPs) are transient windows of heightened plasticity, which are fundamental to the emergence of appropriate network function (Coulson et al., 2022; Dombrovski & Condron, 2021; Hensch, 2004). During a CP, networks display increased susceptibility to activity perturbations, which can result in lasting structural and/or functional changes, while similar perturbations outside the CP are less impactful (reviewed in Coulson et al., 2022, Crisp et al., 2011). The functions and concepts of CPs have traditionally been investigated in the visual system of mammals (Hensch, 2005; Hensch & Quinlan, 2018; Hubel & Wiesel, 1970) and imprinting of birds (Hess, 1975; Horn, 2004). More recently, CPs have also been identified and investigated across a range of species and neuronal ensembles, from networks underlying the development of speech (Harrison et al., 2005) to motor behaviour of rats (Soiza-Reilly & Azcurra, 2009), fish (Hageter et al., 2023) and insects (reviewed in Dombrovski & Condron, 2021; Giachello & Baines, 2015). The presence of a CP in developing networks is therefore increasingly considered a universal phenomenon. The precise changes within networks and associated mechanisms, as they occur during normal development, as well as those resulting from perturbations during a CP, are currently not well understood. This is in large part due to the considerable complexity of the neuronal networks that have been the predominant models for studying CPs, namely mammalian cortical systems.

To overcome this logistical obstacle, we utilize the nervous system of the fruit fly larva, *Drosophila melanogaster*, as a comparatively simpler model with which to study CPs. Though an insect, *Drosophila* also displays CPs whose features suggest commonalities to CPs studied in mammals (for review see Coulson et al., 2022). Currently, the best characterised CP during *Drosophila* development is one that occurs during embryogenesis, which is associated with the larval locomotor network and is linked to the emergence of normal crawling behaviour (Carreira-Rosario et al., 2021; Coulson et al., 2022; S. Crisp et al., 2008; S. J. Crisp et al., 2011; Fushiki et al., 2013; Giachello et al., 2021; Giachello & Baines, 2015; Hunter et al., 2024; Williamson et al., 2021; Zeng et al., 2021). Focusing on this embryonic CP also allows us to take advantage of the comprehensively annotated connectome of the *Drosophila* larval nervous system (Giachello et al., 2020; Valdes-Aleman et al., 2021; Winding et al., 2023) as well as an unparalleled set of genetic tools for manipulating identified neurons with both spatial and temporal precision. Combined with imaging and electrophysiological techniques, this model system enables investigation of the cellular responses to CP manipulations at the level of identified cells and synapses.

Neuronal activity manipulations of various kinds, pharmacological, genetic or optogenetic, when applied during the CP of *Drosophila* embryos, have been shown to cause decreased network stability. This manifests in significantly longer times required for larvae to recover from a strong activity challenge, such as electric shock-induced seizures (Coulson et al., 2022; Giachello et al., 2021; Giachello & Baines, 2015; Hunter et al., 2021, 2024). The premise that balanced network activity during the CP is necessary for stable, resilient networks to form has been explicitly supported by findings from our recent studies. For example, animals mutant for a well-characterized seizure mutation, $para^{bss}$, (expressing hyper-active Na_v sodium channels) are inherently seizure prone. However, transient re-balancing of network activity back to normal levels in $para^{bss}$ mutants, only during the CP, is sufficient to permanently rescue their seizure phenotype (Giachello et al., 2021; Giachello & Baines, 2015; Hunter et al., 2024). By extension, these results also show the therapeutic potential for activity perturbation during identified CPs (Nardou et al., 2023).

While experimental perturbations of neuronal activity during development have been a useful methodological approach for studying CPs as a phenomenon and the associated biological mechanisms, such manipulations might seem artificial in the context of normal development. Most animals are not warm-blooded and in

poikilothermic animals, such as *Drosophila,* changes in ambient temperature, daily as well as seasonal, lead to changes in behavioural activity, likely caused by changes in neuronal and network activity (Lee & Montell, 2013; Powsner, 1935). Studies from the crustacean stomatogastric nervous system show that these minimal networks produce a characteristic, rhythmic firing pattern, which is robustly maintained across a range of external temperatures. However, depending on the annual temperature crabs were harvested, neuronal network properties are accordingly adapted, resulting in a variable "crash temperature" with a difference of almost 10°C (animals caught in 2006: 27°C *vs* animals caught in 2021: 39°C) (Marder, 2023; Marder & Rue, 2021). In *Drosophila,* the temperature experienced by late embryos determines the crawling speed and social feeding behaviour during larval stages (Williamson et al., 2021). Similarly, studies on the *Drosophila* adult visual and olfactory systems showed that neuronal wiring properties and associated behaviours of adults are determined by the temperature experienced during the second CP of *Drosophila,* which takes place during pupariation (Kiral et al., 2021; Züfle et al., 2023), a phase of extensive network remodelling (Lowe et al., 2023).

In this study, we investigated ambient temperature as an ecologically relevant stimulus. To gain insights at the level of single, identified connected cells, we focused on the neuromuscular system of the *Drosophila* larva, and discovered that different components of this network respond differently to transient heat stress, when experienced during the CP. Specifically, we find that increasing temperature increases neuronal activity, and that transient heat stress during the locomotor CP causes long term reduced network stability, similar to the effects of neuronal activity manipulations (Giachello et al., 2021; Giachello & Baines, 2015; Hunter et al., 2024). These changes are accompanied by presynaptic terminal overgrowth at the neuromuscular junction (NMJ) and changes in postsynaptic neurotransmitter receptor composition, though synaptic transmission is homeostatically regulated and remains normal. In contrast, within the central circuitry, we find that transient heat stress leads to reduced excitability of motoneurons, potentially as a response to enhanced synaptic drive from premotor interneurons. Overall, this study presents a first comprehensive analysis of how several interconnected elements of a defined locomotor network develop differently in response to CP perturbation by heat stress, an ecologically relevant stimulus.

Results

Temperature manipulation during the locomotor CP leads to an unstable crawling network

We had previously identified a CP of nervous system development in late embryogenesis, from 17 – 19 hrs after egg laying (AEL), equivalent to 80-90% of embryonic development (Giachello & Baines, 2015). Perturbation of network activity during this time window, for example pharmacologically or optogenetically, leads to the formation of an unstable, seizure prone network. These effects manifest most clearly upon acute activity challenges. For example, an electric shock administered to late larvae, that several days previously had experienced a transient activity manipulation during their embryonic CP, cause seizures with recovery times that are significantly longer compared to unmanipulated controls. Clearly, such large-scale activity manipulations during the embryonic CP are artificial. We wondered, therefore, to what extent environmental conditions, that embryos might normally encounter during this CP, might also alter locomotor circuit development. As poikilothermic animals, *Drosophila* development strongly depends on ambient temperature (Powsner, 1935), and several studies have shown that temperature experiences during development alter neuronal wiring as well as behaviours in larval and adult flies (Kiral et al., 2021; Williamson et al., 2021; Züfle et al., 2023).

We exploited heat stress of 32°C (Scialò et al., 2015), which is known to be experienced by *Drosophila melanogaster* (Williamson et al., 2021), i.e. 7°C above the evolved temperature preference of 25°C (Ashburner et al., 1983). We exposed embryos to 32°C before, during, or after the CP, and measured the speed of recovery from electric shock-induced seizures, as a proxy for network stability. Applying transient heat stress before or after the CP did not result in less stable networks (i.e. no change in seizure response), while 32°C heat stress during the CP significantly increased the recovery time from induced seizure, indicative of reduced network stability (Fig. 1A). Several studies have shown that increasing temperature leads to increased activity in the locomotor network (Oswald et al., 2018; Sigrist et al., 2003; Zhong & Wu, 2004). We tested this by measuring spontaneous calcium transients from aCC motoneurons (in isolated CNS), expressing GCaMP8f selectively in aCC motoneurons under the control of R94G06-GAL4. Stepwise increases in temperature

correlate with both, and increase in GCaMP signal amplitude and frequency of rhythmic bursts, whereas CNSs kept at 25°C for the functional imaging duration tended to show decreasing neuronal activity (Fig. 1B). These experiments suggest that increases in ambient temperature, over 25ºC, lead to concomitant increases in locomotor network activity. When those occur during the embryonic CP, they result in different developmental outcomes, namely of less stable networks.

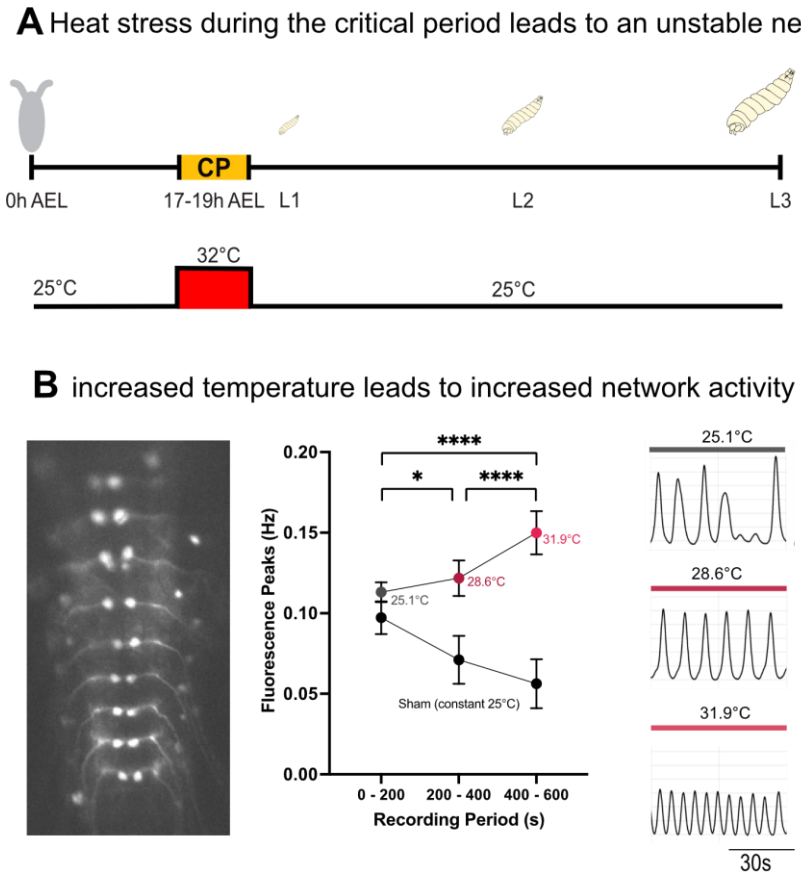

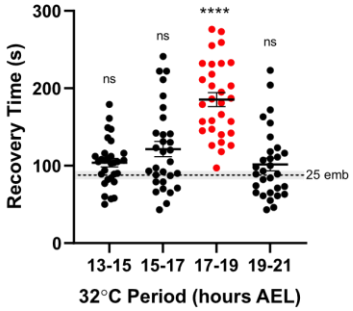

Figure 1: Transient heat stress during the critical period leads to unstable networks

A Schematic representation of embryonic and larval development and temperature manipulation during embryogenesis. Embryos were kept at 32°C for 2 h either before (13-15 h, 15-17 h AEL), during (17-19 h AEL) or after (19-21 h AEL) the locomotor network CP. **B** Acute increase of temperature leads to increased network activity, as measured with the fluorescent calcium indicator GCaMP8f expressed in segmentally repeated aCC motoneurons in isolated central nervous systems; while constant 25°C leads to reduced activity over time.

Temperature manipulation during the locomotor CP leads to lasting change in NMJ morphology

We have documented that activity manipulation (pharmacological) during the embryonic CP can manifest in lasting synaptic change within the central locomotor circuitry (Hunter et al., 2024). Here, we have taken advantage of the well characterised, and easy to access, peripheral neuromuscular junction (NMJ) to test, with single cell resolution, structural and/or functional change that result from CP perturbation. We focused on the NMJ of dorsal acute muscle 1 (DA1), which is innervated by the aCC motoneuron (Fig. 2A) (Baines et al., 1999, 2001; Fujioka et al., 2003; Landgraf et al., 2003) and screened for morphological changes after transient embryonic CP temperature manipulation. Because temperature manipulations outside the CP did not lead to an unstable network (Fig. 1A), we adapted the experimental paradigm to put embryos from a 6h egg collection to 32°C for 24h, to make sure all embryos went through their CP, while experiencing the heat stress. Focusing on the excitatory Ib boutons of the aCC motoneuron we could show that after a 32°C CP manipulation, the presynaptic terminals on muscles of late L3 larvae are significantly overgrown (quantified for the aCC-DA1 NMJ; HRP in green) resulting in an increase in bouton number and active zones (magenta), while overall active zone density is not altered (Fig. 2B). On the postsynaptic side, embryonic CP heat stress causes an altered receptor composition: a selective reduction of the larger conductance GluRIIA subunit, which leads to an overall reduced ratio of the larger conductance GluRIIA *versus* the lower conductance GluRIIB subunit (Fig. 2C-Cii).

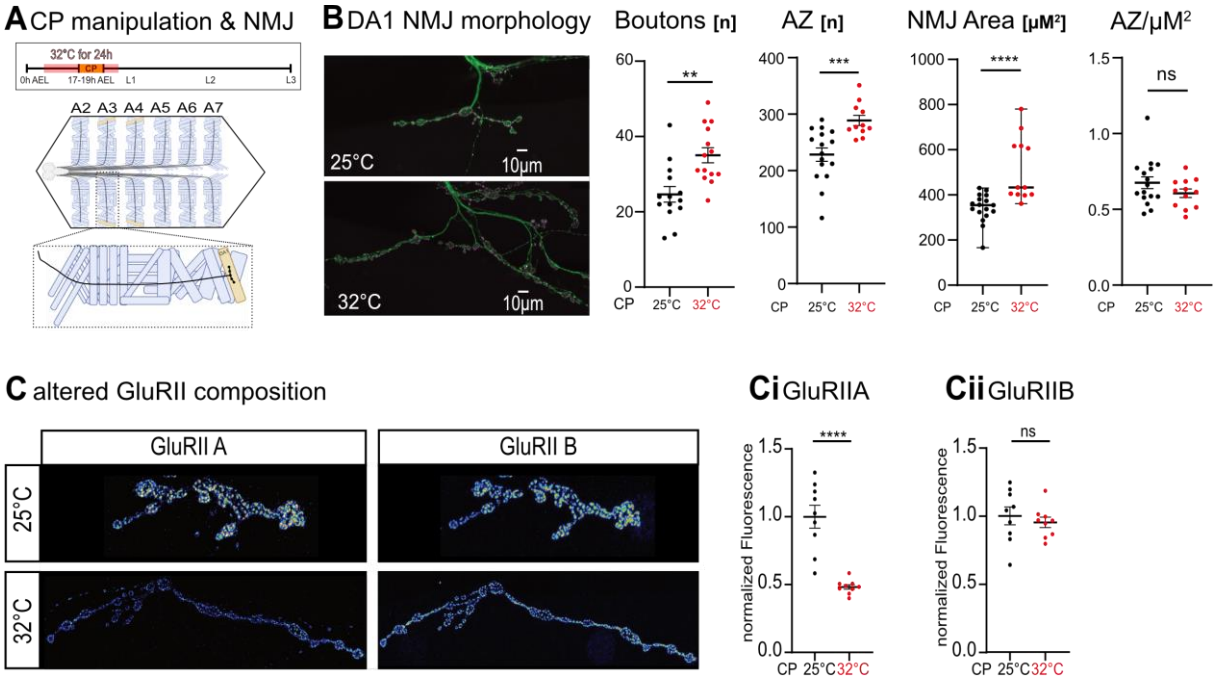

Figure 2: Morphological changes at the neuromuscular junction after critical period perturbation. A Schematic of temperature manipulation during embryogenesis and the dorsal acute muscle 1 (DA1) within a fillet dissected larva. After a 6h laying period, embryos were kept at 32°C for 24h to guarantee a manipulation during the neuronal critical period. **B** Temperature manipulations as depicted in A, result in a significant overgrowth of aCC presynaptic terminals at the NMJ and an increase in bouton numbers and NMJ area. A concomitant increase in active zone number (magenta) results in a normal active zone density. **C** postsynaptically, critical period temperature manipulations result in a decrease of glutamate receptor A **(Ci)** while glutamate receptor B remains unaffected **(Cii).**

Despite morphological changes, NMJ physiology is not altered

In view of the prominent changes in NMJ growth, morphology and postsynaptic glutamate receptor composition that result from heat stress (32°C) during the embryonic CP, we next assessed synaptic physiology at this NMJ. To this end, we used the two-electrode voltage clamp (TEVC) technique, initially measuring single pulse transmission across a gradient of external calcium concentrations. Despite the marked structural changes in manipulated animals, single pulse transmission is not significantly different between embryonically manipulated (32°C experience during their CP) and controls that experienced 25°C throughout (Fig. 3 A&B). Quantifying the number of release sites utilised per action potential and quantal size (Jusyte et al., 2023) also showed no statistically significant difference between CP-manipulated and control specimens (Fig. 3C). Next, we quantified the size of the readily releasable pool of synaptic vesicles by recording responses to a high frequency train of action potentials (Fig. 3D), then plotting the cumulative amplitude of responses to the first 60

pulses and linearly back extrapolating through the last 20 pulses to y=0 (Fig. 3E). This also did not show a significant difference between CP-manipulated and control animals (Fig. 3F). However, we noticed that during the 60Hz pulse train, NMJs in CP-manipulated specimens exhibited an increased facilitation during the first 10 pulses, indicating a slight reduction in release probability of the presynaptic terminal (Fig. 3D). Finally, we tested if the NMJ is still able to adjust homeostatically for acute changes to synaptic transmission. We utilized the well-established method of acutely blocking glutamate receptors with Philanthotoxin (PhTx), a GluRIIA blocker, to induce presynaptic homeostatic potentiation (Frank et al., 2006; Genç & Davis, 2019; Müller & Davis, 2012). Establishing baseline conditions, we found no difference in mEPSC amplitude between controls and CP-manipulated animals, or quantal content Fig. 3G-Giii). This is contrary to what we had expected given the overall reduction in the DGluRIIA/B ratio in CP-manipulated specimens. However, we noticed that reductions in DGluRIIA signal were most pronounced in proximal regions of the NMJ, while distal boutons, which have a high probability of release under low frequency stimulation regimes (Peled & Isacoff, 2011), have normal levels of DGluRIIA signal and could thus explain the lack of effect on mEPSC amplitude. Acute GluRIIA blockade by a 10 min incubation with PhTx caused a significant reduction mEPSC amplitude while evoked EPSC amplitude remained unchanged in both controls and CP-manipulated specimens. Calculating quantal content shows that in response to acute GluRIIA blockade, both control and CP-manipulated animals are indeed able to induce presynaptic homeostatic potentiation by increasing quantal content (Fig. 3G-Giii). Thus, we conclude that despite the significant structural change caused by a transient embryonic 32°C heat stress experience days earlier, synaptic physiology at the NMJ remains normal.

Even though the NMJ does not show significant changes in physiology, we noticed that in CP-manipulated specimens, motor axons required increased stimulation voltage to reliably induce action potentials. This hints at motoneurons in CP-manipulated larvae having acquired reduced excitability. Together with the above observation of a slightly reduced release probability and reduced postsynaptic GluRIIA, it seems that following CP manipulation, individual parts of the crawling network have homeostatically adjusted to maintain normal evoked synaptic transmission at the NMJ, most likely to maintain robust motor output. Conversely, when considering the unstable network phenotype, as manifest by increased recovery times from electric shock-induced

seizures, our findings of normal synaptic transmission at the NMJ suggests that network instability likely originates from changes within the central locomotor circuitry.

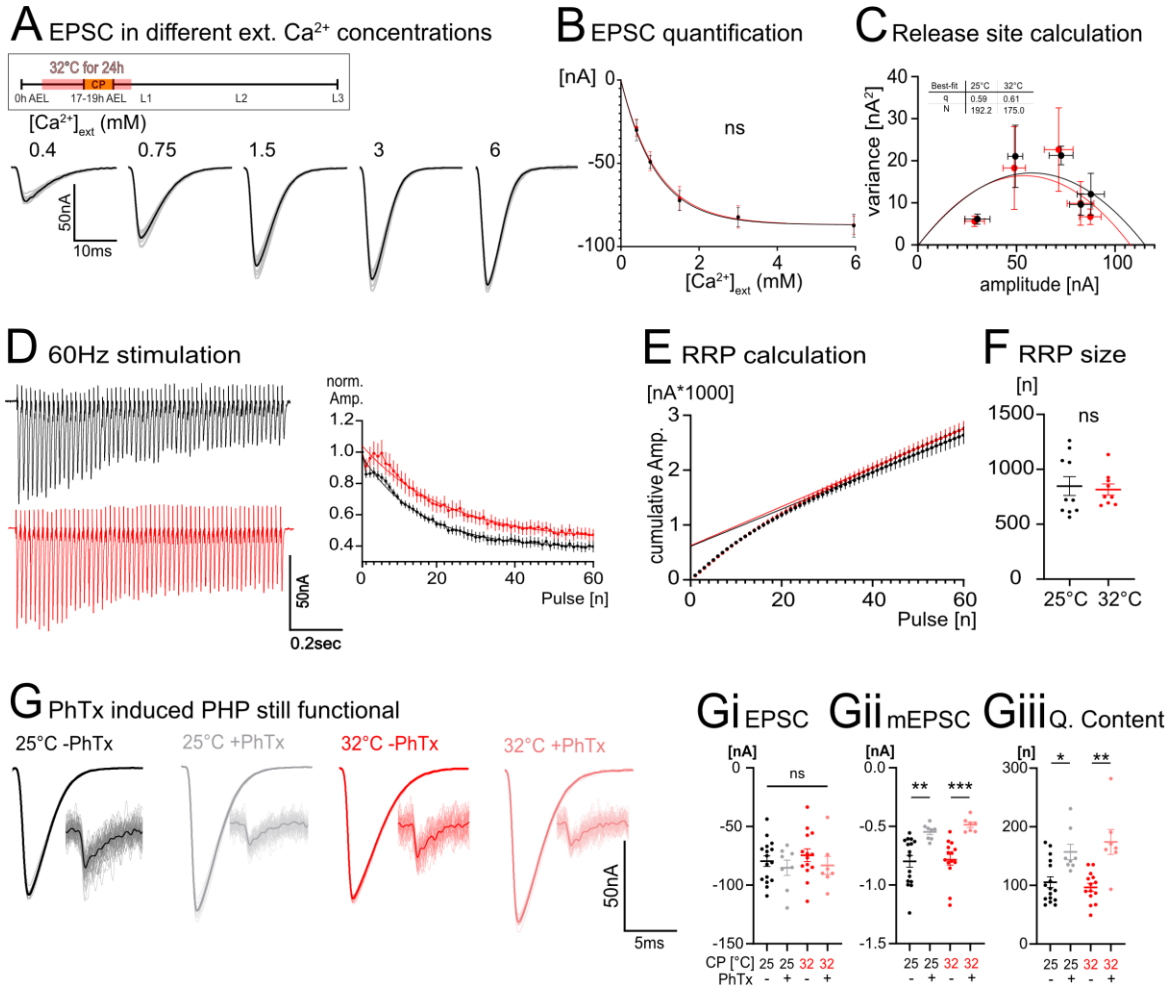

Figure 3: Physiological NMJ properties after 32°C perturbation. A Representative traces of control two electrode voltage clamp recordings across a gradient of external calcium concentrations. **B** Postsynaptic current amplitude is not altered between control and CP-manipulated animals at any given external calcium concentration. **C** plotting postsynaptic current amplitude against its variety to calculate quantal size (q) and the number of release sites being used (N), also did not show a significant difference between control and CP-manipulated animals. To measure readily releasable pool size, a 60Hz stimulus train was applied for 1s **(D)** where we could observe a slight increase in facilitation over the first 10 pulses in specimens that in their embryonic stage had experienced heat stress of 32°C. Cumulative amplitude was plotted over time and a linear regression was back extrapolated through the last 20 pulses **(E)**. The y intercept was divided by the Mini size of the same trace to calculate the readily releasable pool size. **G-Giii** NMJs in CP-manipulated specimens have normal EPSC and mEPSC amplitudes and quantal content. Acute application of the GluRIIA blocker PhTx reliably induced presynaptic homeostatic potentiation in controls and 32°C CP-manipulated animals.

Motoneurons display reduced excitability upon increased synaptic input in response to embryonic heat stress

Having noticed a potential reduction in motoneuron excitability in late larvae that, as embryos, had experienced 32°C heat stress, we set out to directly test motoneuron excitability. To this end, we used whole cell patch clamp to measure evoked action potential firing, as a measure of excitability of the aCC motoneuron. These measures were made in the presence of mecamylamine (200 μM in external saline) to block endogenous cholinergic excitatory synaptic drive. Action potential firing of aCC was evoked using injection of current steps (4pA). We found that in late L3, aCC had significantly decreased excitability following an embryonic CP experience of 32°C heat stress (Fig. 4A). These results are comparable to, and also validate, results obtained after optogenetic locomotor network activity manipulation during the same embryonic CP (Giachello & Baines, 2015). In previous studies, we had shown with recordings from aCC that its synaptic drive is enhanced following transient CP manipulations of network activity, using optogenetic or pharmacological means to induce network over-excitation, or genetic overactivation of neurons, as in *para*^{bss} seizure mutants (Giachello & Baines, 2015; Hunter et al., 2024). Specifically, endogenous excitatory cholinergic synaptic currents, termed spontaneous rhythmic currents (SRCs), were increased in duration, though not in amplitude, as a result of those CP network activity manipulations (Giachello et al., 2019; Giachello & Baines, 2015). We asked if heat stress during the CP led to similar changes. Indeed, in late larvae that had transiently experienced heat stress during their embryonic CP, SRCs from aCC motoneurons were significantly increased in duration, though with amplitude unchanged (Fig. 4Bi). Note these SRC recordings were undertaken in the absence of mecamylamine. The above observations, including the decrease in membrane excitability of aCC, are compatible with the idea of motoneurons having undergone homeostatic adjustment in response to increased pre-motor excitatory synaptic drive.

To test that hypothesis, we recorded synaptic drive to aCC, under whole cell patch clamp configuration, while optogenetically activating a specific and strongly connected excitatory premotor interneuron, termed “A27h” (Hunter et al., 2023). Because motoneurons are quiescent without synaptic drive, a small amount of current was injected to aCC to maintain a modest and consistent mean firing frequency of ~10-20 Hz. As might be expected, and as per our previous study (Hunter et al., 2023), acute optogenetic activation of the A27h premotor excitor resulted in increased aCC firing

frequency. Significantly, however, this increase was greater in larvae that as embryos had been exposed to heat stress during the CP than in control specimens (Fig 4.Bii). This observation supports the hypothesis that heat stress during the embryonic CP results in increased excitatory drive from central interneurons, which is then countered by reduced excitability in postsynaptic motoneurons.

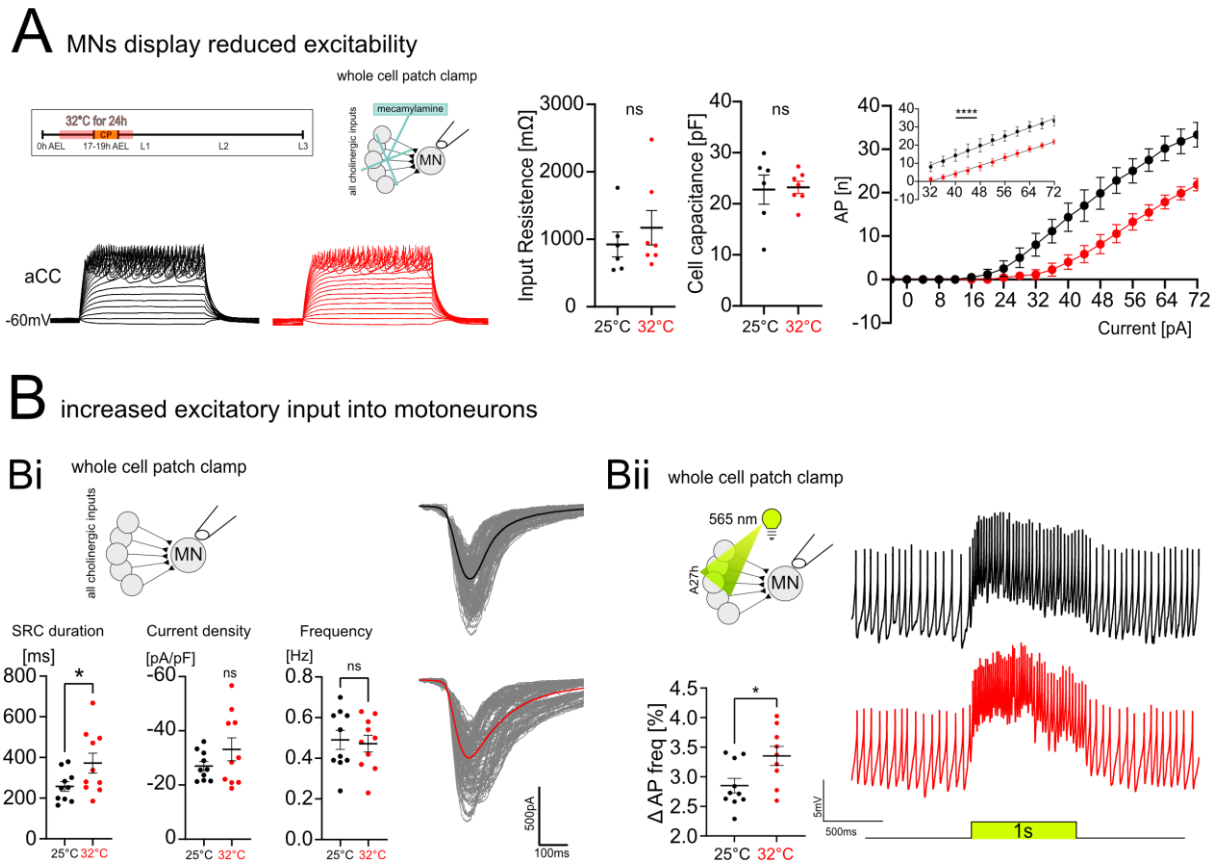

Figure 4: Larval motoneurons display reduced excitability and increased synaptic input after an embryonic 32°C CP-manipulation. A aCC motoneurons at the late third instar larval stage, isolated from excitatory synaptic input. Motoneurons in specimens, which during the embryonic CP had transiently experienced 32°C heat stress, show significant reduction in excitability relative to controls. **B** Left: whole cell patch clamp recordings from the aCC motoneuron reveal an increase in spontaneous rhythmic current duration several days after embryos had experienced transient 32°C heat stress during the CP. Right: targeted optogenetic activation (using Chronos) of a pre-motor excitatory interneuron (A27h) showed that A27h input is increased in late larvae that as embryos had experienced 32°C heat stress during the CP.

Homeostatic adjustments of the aCC motoneuron result in normal endogenous firing patterns

Thus, if the adjustments displayed by the aCC motoneuron are indeed a homeostatic response, then one might predict this to be a mechanism to maintain the endogenous level of motoneuron activity. To test this idea, we used whole cell patch recordings from aCC motoneurons from isolated nerve cords of late third instar larvae. As hypothesized, our recordings show no significant differences resulting from embryonic CP heat stress experiences; in endogenous motoneuron activity, as measured by burst rate, burst duration, or action potentials per burst (Fig. 5A). Finally, to test if homeostatic adjustments of motoneurons translate to normal muscle output, we recorded spontaneous synaptic drive from muscles in a semi-intact preparation with an attached, intact nervous system. Current clamp recordings from the DA1 muscle, while supressing muscle contractions using nifedipine (50µM) (Dyson et al., 2022; Kratschmer et al., 2021), showed no significant differences in spontaneous burst frequency or duration, nor the overall time spent bursting (Fig. 5B), between controls and CP heat stress-manipulated specimens. Therefore, we conclude that CP manipulations act primarily on the cells of the pre-motor circuitry, namely excitatory pre-motor interneurons as tested in this study, while changes in the motoneurons can be seen to constitute homeostatic adjustments in response to those primary pre-motor network changes.

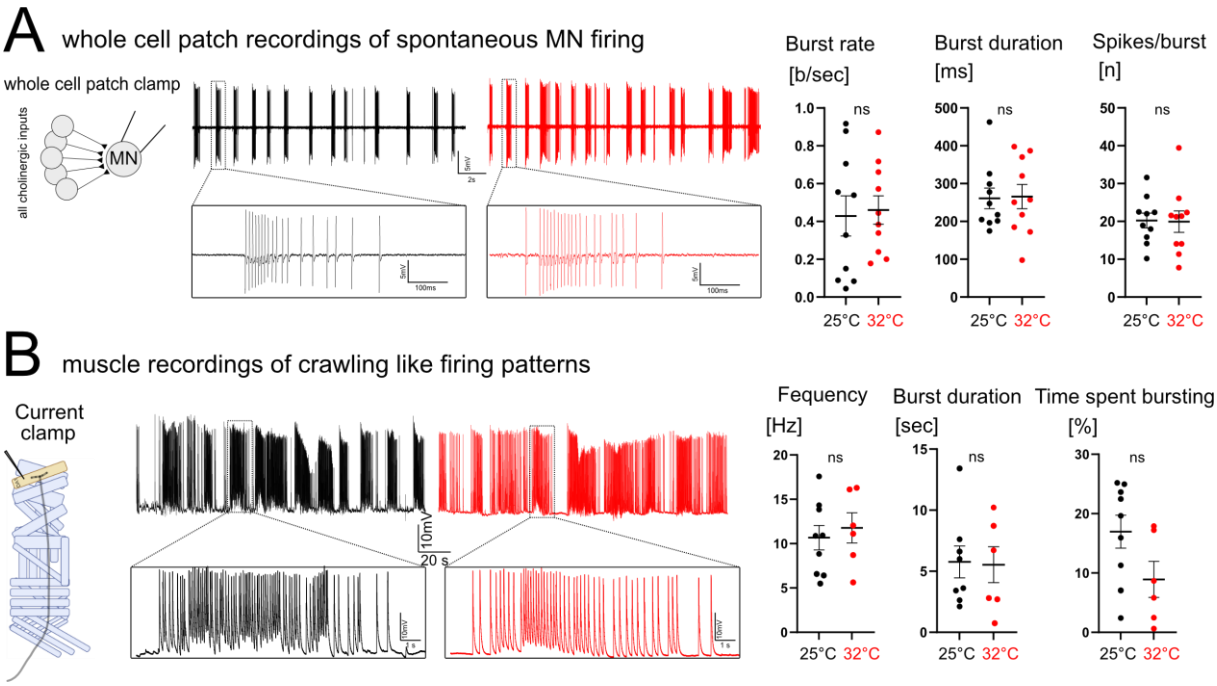

Figure 5: Spontaneous larval motoneuron and muscle firing properties and are unchanged after embryonic temperature challenge. A Monitoring spontaneous firing by loose cell patch clamp recordings from the aCC

motoneuron in a late third instar larval nerve cord did not show a significant difference between CP-manipulated specimens and controls. **B** Measuring muscle output of motoneuron spontaneous firing by current clamp recordings from the DA1 muscle in late third instar larvae showed that animals are able to produce normal motoneuron firing output to the muscle, irrespective of embryonic experience.

Interneurons display increased inter-segment wave propagation upon 32°C critical period manipulation

To test how excitatory premotor interneurons are affected upon 32°C critical period manipulation, we expressed the calcium indicator GCaMP8f in A27h interneurons in isolated 3rd instar nerve cords and recorded wave propagation from abdominal segments A6-A1 (Fig.6A). These experiments show that the timing of wave propagation in pre-motor interneurons is significantly decreased in larvae, which experienced 32°C during their CP, compared to untreated controls. Finally, we asked how a CP-induced decrease in wave propagation might translate to decreased crawling speed (Fig.6B). As our electrophysiological analyses showed, motoneuron firing patterns and output to the muscle remain normal after a 32°C CP manipulation (Fig.3-5). These results further support the hypothesis that network instability after such a CP manipulation originate from the premotor interneurons, rather than from motoneurons.

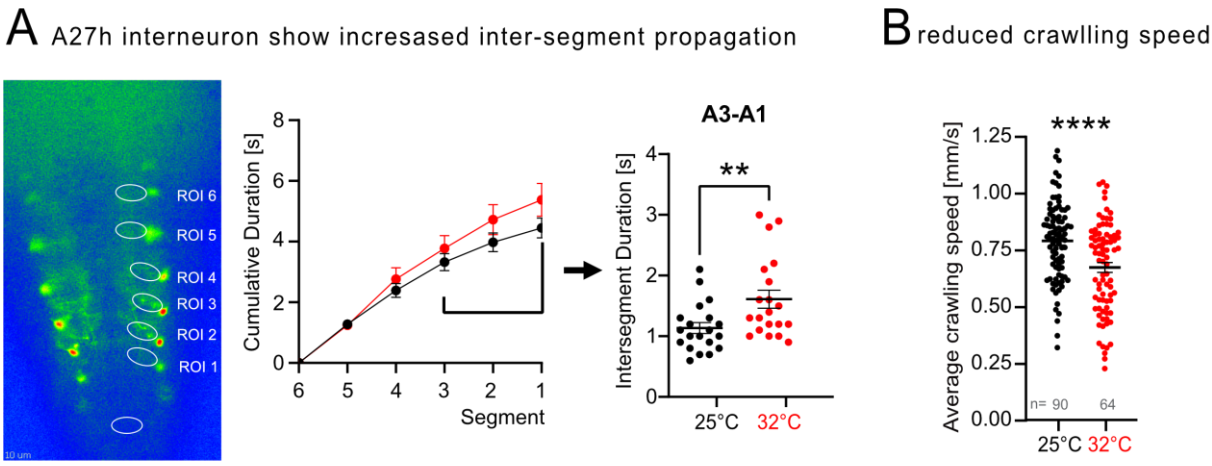

Figure 6: Larval interneurons display increased intersegment duration after an embryonic, together with L3 larva exhibiting reduced crawling speed 32°C CP-manipulation. A Calcium imaging of A27h interneurons using GCaMP8f. At late third instar, dissected CNSs from larvae that had experienced transient 32°C heat stress during the CP, showed increased intersegment duration between segments A3 and A1. **B** Assaying larval network activity by larval crawling speed reveals a decrease in crawling speed in larvae which were exposed to 32°C during their CP, compared to controls.

Discussion

An experimental model system with which to study CP biology

In this study we have utilised the larval neuromuscular system as an experimental model with which to study the role of CP-regulated plasticity across interconnected cells within a defined circuit. We have identified 32°C heat stress as an ecologically relevant CP stimulus: transient exposure of embryos to 32°C during the previously defined CNS CP (17-19 hours after egg laying), though not before or after this developmental window, leads to lasting changes in subsequent nervous system development, resulting in an increased susceptibility to electro-shock induced seizures. Calcium imaging of motoneurons demonstrated an increase of rhythmic locomotor network activity upon stepwise increases in ambient temperature. This is in line with past studies, which had demonstrated the well-established link between temperature and neuronal activity, also in this specific experimental system (Zhong & Wu, 2004). It is, therefore, not surprising that 32°C heat stress during the embryonic CP of nervous system development causes comparable outcomes to other neuronal activity manipulations (pharmacological or genetic) during this developmental window (Giachello et al., 2021; Giachello & Baines, 2015; Hunter et al., 2024).

Different cell types respond differently to CP manipulations

A particular strength of this system is the accessibility of interconnected network elements. We focused on a small part of the locomotor network, a short chain of an excitatory pre-motor interneuron (A27h) connected to a motoneuron (aCC), and its postsynaptic target body wall muscle (DA1). Following transient application of heat stress as an ecologically relevant, systemic stimulus during the embryonic CP, we could identify that within this section of the locomotor network each of these three connected nodes responds differently. We observed increased excitatory drive from A27h interneurons, while motoneurons displayed homeostatic adaptation; namely, a decrease in excitability, resulting in normal firing patterns. At the presynaptic NMJ terminal in the periphery, in contrast, we documented normal synaptic transmission properties, despite a significant increase in bouton number. The latter might be a secondary adjustment to a decrease in transmitter sensitivity (reduced DGluRIIA levels) by the muscle.

The first observation to make is that the responses have been reproducible, suggesting that either there are direct cause-effect relationships at the cellular level, which can now be investigated in detail or, alternatively, activity patterns in this part of the network are robustly canalised to effect predictable outcomes. Second, the changes in neuronal excitability and synaptic transmission are compatible with a temporal sequence, or a functional hierarchy, during network maturation. For example, following an embryonic heat stress, pre-motor interneurons, potentially part of the central pattern generator (Carreira-Rosario et al., 2021; Zeng et al., 2021), increase their collective synaptic drive to the (aCC) motoneuron, which in turn exhibited reduced excitability (Figure 4). Thus, the motoneuron might have responded homeostatically to the increase in presynaptic excitatory drive. It further implies a hierarchy, whereby the specification of premotor interneuron properties dominates that of their downstream integrators, the motoneurons. To test if this was indeed the case, future studies should investigate the temporal sequence of events by which cellular and synaptic properties change after a CP perturbation; asking whether the properties that we have recorded at the late 3rd instar larval stage are arrived at directly, or over a long period, indicative of a change in developmental trajectory, or perhaps indirectly, e.g. in the event that a CP activity perturbation caused non-linear or oscillatory effects, which were canalised by the network dynamics into cell type-specific outcomes.

NMJ development but not synaptic transmission is affected by CP manipulations

That the motoneuron-muscle synapse retains normal synaptic transmission properties, might have been expected. Though the details of how this is achieved are unclear. Despite significant structural changes resulting from an embryonic heat stress, in terms of presynaptic terminal overgrowth (an average increase of active zones number by 30%) and overall reduced DGluRIIA amount (by 50%) evoked transmission upon single action potentials is normal. Close inspection suggests that DGluRIIA distribution is no longer homogenous in late larval NMJs if the animal had experienced heat stress during its embryonic CP, with DGluRIIA levels reduced proximally (axon entry point) but at control level in distal boutons. Distal boutons had previously been demonstrated to house release sites that are preferentially recruited under low frequency stimulation regimes, which could explain our observations (Peled & Isacoff, 2011). If this was the case, then one might expect high frequency stimulation regimes, e.g. of 60 Hz, to recruit many other presynaptic sites for vesicle fusion, including the proximal sites that are opposed to postsynaptic densities with noticeably reduced DGluRIIA. Although we

did not conduct functional imaging to investigate this directly, a 60 Hz stimulation regime did indeed reveal increased facilitation, indicating a reduction in presynaptic release probability across the whole synapse in response to heat stress during the embryonic CP. Though statistically not reaching significance, this points to changes in release probability that would also be compatible with the idea that at sub-60 Hz stimulation a much larger fraction of synaptic release sites are recruited, including proximal, low DGluRIIA sites (Figure 3D). That evoked synaptic transmission at the NMJ is not significantly affected by CP manipulations, is perhaps to be expected. A well-established feature of this synapse is that its transmission is tightly regulated in order for it to maintain consistency. The various NMJ plasticity mechanisms include presynaptic homeostatic potentiation (PHP), which we have shown to function effectively, also after CP heat stress manipulation (Delvendahl & Müller, 2019; Frank et al., 2006, 2020; Goel & Dickman, 2021).

It is unlikely that these structural changes at the NMJ have any contribution to making the nervous system less stable in the face of strong stimuli. Whether and how CP-regulated adjustments at the NMJ might contribute to other temperature experience-regulated behaviours, such as larval crawling and social feeding, remains to be seen (Williamson et al., 2021). Based on previous motoneuron-targeted CP manipulations (Giachello et al., 2021), it seems more likely that the behavioural consequences that we see, including reduced crawling speed and increased recovery times from electric shock-induced seizures, would be effected by changes in central circuitry.

Nevertheless, having established clear, quantifiable structural responses to embryonic CP manipulations, this large, readily accessible peripheral synapse could be used to identify genetic pathways required for sensing growth conditions during the CP, and for implementing changes in subsequent development. For example, the changes in growth, active zone numbers and postsynaptic receptor field composition that we have detailed here would make for a differentiated readout of developmental changes in response to CP perturbations. Those are well suited for genetic approaches, from enhancer-suppressor screens to epistasis experiments. From a network perspective, motoneurons and muscles constitute the output of the locomotor system and in this system happen to be exclusively postsynaptic. By not being highly interconnected with a wider network, as is the case for most central neurons, working with motoneurons and muscles could be advantageous for studying cause-effect relationships of CP manipulations. This could be particularly advantageous for examining the question of

how the severity of CP perturbations relates to resultant long-term adjustments. Furthermore, it will be of interest to future research, to what extent we can transfer insights from single cell level about critical period adjustments and homeostatic adjustments to network wide adjustments. As we could show, acute temperature increase leads to faster rhythmic activity, but we record reduced speed of wave propagation in A27h interneurons in L3 larvae after CP manipulation. This could either be caused by a malfunctioning pacemaker activity due to critical period perturbation or slowing of the CPG is network wide homeostatic response to what is perceived a too fast a rate during the CP.

Acknowledgements

This work was made possible through support by a Walter Benjamin Programme Fellowship to NK by the Deutsche Forschungsgemeinschaft (DFG) KR5597/1-1, and funding from the Biotechnology and Biological Sciences Research Council (BBSRC) to ML (BB/V014943/1) and the Wellcome Trust, through a Joint Wellcome Trust Investigator Award to RAB and ML (217099/Z/19/Z). Research reported in this publication was supported by an institutional startup fund from Texas A&M University (AAZ). DSC was supported by the European Molecular Biology Organization (EMBO) with a long-term EMBO fellowship (ALTF 62-2021). The work benefited from the Imaging Facility, Department of Zoology, supported by Matt Wayland and Tom Pettini, and funds from a Wellcome Trust Equipment Grant (WT079204) with contributions by the Sir Isaac Newton Trust in Cambridge, including Research Grant [18.07ii(c)]. Work on this project further benefited from the Manchester Fly Facility, established through funds from the University and the Wellcome Trust (grant 087742/Z/08/Z).

The authors would like to thank members of the Baines and Landgraf research teams for feedback on the manuscript. The authors are grateful to Ela Serpe for Rabbit polyclonal anti-DGluRIIB antiserum.

Stocks obtained from the Bloomington Drosophila Stock Center (NIH P40OD018537) were used in this study.

The 8B4D2 (MH2B) monoclonal antibody, developed C. Goodman, was obtained from the Developmental Studies Hybridoma Bank, created by the NICHD of the NIH and maintained at The University of Iowa, Department of Biology, Iowa City, IA 52242.

Materials and Methods

Fly husbandry

Wild-type and transgenic strains were maintained on standard yeast–agar–cornmeal medium at 25˚C. For CP manipulations, animals were kept in laying pots with apple juice agar plates and yeast paste for 6h. Collected eggs were either kept at 25°C for controls or at 32°C for 24h, before being moved back to 25°C until animals developed to wandering L3 larvae.

Dissection and Immunostainings

Wandering L3 larvae were dissected in Sørensen's sodium phosphate buffered saline (0.1 M, pH 7.2) and fixed for 10min at room temperature with Bouin´s fixative (Sigma-Aldrich). After fixing, specimens were washed in washing solution (Sørensen's buffer + 0,25% BSA + 0,3% TritonX-100 from Sigma-Aldrich) and incubated with mouse nc82 (anti-Bruchpilot to reveal active zones) antibody (1:100, DSHB) overnight, visualized with goat α-mouse StarRed (1:1000, Abberior, cat.no.STRED-1001-500UG, Lot. 2042PK-1) and AlexaFluor488 conjugated goat α-HRP (1:1000, Jackson ImmunoResearch, cat.no. 123-545-021, Lot. 152767) to visualise presynaptic, neuronal structures. For stainings of the postsynaptic glutamate receptor subunits GluRIIA and GluRIIB we used monoclonal mouse-α-DGluRIIA antibody (1:100, DSHB, product ID: 8B4D2 (MH2B)) and polyclonal rabbit-α-DGluRIIB antiserum (1:1000, gift from Mihaela Serpe (Sulkowski et al., 2016)) in conjunction with goat α-mouse StarRed (1:1000) and goat α-rabbit Atto594 secondary antibodies (1:1000, Hypermol, cat.no. 2306, Lot. 0356RG22), respectively, in combinations with AlexaFluor488 conjugated goat α-HRP (1:1000, Jackson ImmunoResearch, cat.no. 123-545-021, Lot. 152767) to visualise presynaptic terminals.

Fly stocks

Genotype	Phenotype	FlyBase identifiers
Oregon-R	Wildtype control	FBst0002376
Canton S	Wildtype control	FBst0064349
w^{1118};;P{y[+t7.7] w[+mC]=GMR94G06-GAL4}attP2	Targets Gal4 expression selectively to the aCC motoneuron during embryonic and larval stages; kindly gifted by Juan J. Pérez Moreno (Pérez-Moreno & O'Kane, 2019).	FBti0139793
w[1118]; PBac{y[+mDint2] w[+mC]=20XUAS-IVS-jGCaMP8f}VK00005	GCaMP calcium imaging	FBti0215881
w[1118]; P{y[+t7.7] w[+mC]=GMR36G02-GAL4}attP2	Expresses Gal4 in A27h and M neurons, plus two ventral cells per hemineuromere, used for calcium imaging	FBti0135233
34F03-AD/CyO;36G02-DBD/TM2	A27h neuron driver used for whole cell patching A27h	
w[*] ; P{y[+7.7] w[+mC]=20UAS-Chronos-mVenus}attP40	Red-shifted channel rhodopsin line used to excite the A27h premotor interneuron to its measure synaptic drive to the aCC motoneuron	FBti0195682

Image acquisition

Confocal images were acquired, using a Leica Stellaris point scanning confocal microscope, with an 40x/1.25N.A. oil immersion lens (Leica) and a 1.25 digital zoom. Images were acquired with a voxel size 0.16x 0.16x 0.3 µm. Images were processed using FIJI and Affinity Designer.

Two electrode voltage clamp

Two Electrode Voltage Clamp (TEVC) recordings were performed in HL3.1 saline (Feng et al., 2004) composition in mM: NaCl 70, KCl 2.5, $MGCl_2$ 4, $CaCl_2$ 2 (if not other mentioned), $NaHCO_3$ 10, trehalose 5, sucrose 115, HEPES 5 (pH was adjusted to 7.24-7.25 with 1M NaOH), using an Olympus BX50WI compound microscope with 60X dipping (Olympus 60x/0.9 N.A.) objective lenses. Experiments were performed on third-instar larval NMJs of the dorsal acute muscle 1 (DA1) in segments A3 and A4. The respective nerve was sucked in with a self-built suction electrode (Johnson et al., 2007) which was filled with HL3.1 saline. Subsequently, the nerve was stimulated for 0.1ms to trigger action potential firing. Briefly, voltage was stepwise increased until the first synaptic transmission could be recorded. From that voltage, 1 V was added to reliably evoke APs in control conditions, in 32°C CP manipulated animals 2-3 V had to be added to reliably recruit aCC and RP2. For PhTx experiments, samples were incubated in 4 µM PhTx final concentration (Frank et al., 2006) for 10 min. While dissecting, great care was taken to not stretch animals too much. Successful PhTx application was determined by dividing miniature EPSC amplitude of PhTx treated animals by the average Amplitude of control mEPSCs. If PhTx treated mEPSCs were at least 40% reduced compared to control, PhTx application was considered successful (Frank et al., 2006). Quantal content was determined by dividing EPSC by mEPSC for each recording. Recordings were only further considered from cells with an initial Vm below -50 mV and input resistance between 8-10 MΩ, using intracellular electrodes filled with 3M KCl with resistances of ~20 MΩ (Electrodes for current injection and the membrane voltage). Current passing und recording electrodes were pulled from Borosilicate glass microelectrodes with filament (OD1 mm, ID 0.58mm; Harvard Apparatus LTD, GC100F-10 Part No. 30-0019), suction electrodes from Borosilicate glass microelectrodes without filament (OD1 mm, ID 0.58mm; Harvard Apparatus LTD, GC100-10 Part No. 30-0016) with a Flaming/Brown Puller Model P-97 (Sutter Instruments USA). Excitatory postsynaptic currents (EPSCs) were evoked by an Isolated Pulse Stimulator (Model 2100 A-M Systems USA), recorded at a clamped voltage of -60 mV with a sampling rate of 50 kHz and filtered with the anti-alias filter at 25 kHz using the AxoClamp 2B amplifier (Molecular Devices Axon Instruments USA). Data analysis was done with Clampfit 10.7. Traces were first filtered with a 360 Hz Gaussian low pass filter, then template searches were run over the trace for single pulses and spontaneous miniature excitatory postsynaptic currents (mEPSCs or

minis). The resulting files were used to analyse mEPSC and EPSC properties. Rise and decay tau were measured with an one-term exponential product fit (Levenberg-Marquadt method with a max of 5000 iterations)

Current clamp muscle recordings

Current clamp recordings from muscle DA1 were performed in HL3.1 saline (see above), in semi intact, fillet dissected wandering L3 larvae with intact nervous system. After finishing the dissection, only animals performing crawling-like movements were considered for further experiments. To block muscle contractions, a 500 μM stock solution of nifedipine in HL3.1 and 1% DMSO was added to the bath for a final concentration of 50 μM nifedipine and 0.1% DMSO for 15 min. Recordings were only further considered from cells with an initial Vm below -60 mV and input resistance between 8-10 MΩ, using intracellular electrodes filled with 3M KCl with resistances of ~20 MΩ. Spontaneous activity was recorded for 5min. Burst analysis was performed using the Clampfit Burst Analysis, using the Poisson Surprise model with a minimum of 5 events per burst.

Electroshock assay

A handheld stimulator consisting of two tungsten wires (0.1 mm diameter) fixed to a plastic rod was used. Wires were shaped to be ~1-2 mm apart, attached to a DS2A Mk.II stimulator (Digitimer Ltd), which was set to provide a 6 V, 2 s current pulse. Larvae were placed on a plastic plate lid, with tissue paper used to dry residual moisture from the larvae. Once larvae had returned to normal crawling, the tungsten wires were brought into contact with the larvae, positioned on the larval cuticle, perpendicular to and over the approximate position of the CNS, with gentle pressure. Current stimulation was then delivered, which usually induced a sustained contraction and paralysis representing a seizure (videos can be viewed in Marley and Baines 2011). The time to resumption of normal behaviour (regular, whole body forward propagating peristaltic waves) was recorded and defined as the duration of recovery from seizure.

Dissection and CNS mounting for calcium imaging and electrophysiology

Larval CNSs were dissected and mounted for electrophysiological recordings and for GCaMP imaging. Third instar (L3) larvae (of either sex) were dissected in a dish in standard saline (135 mM NaCl (Fisher Scientific), 5 mM KCl (Fisher Scientific), 4 mM $MgCl_2 \cdot 6H_2O$ (Sigma-Aldrich), 2mM $CaCl_2 \cdot 2H_2O$ (Fisher Scientific), 5 mM TES (Sigma-Aldrich), 36 mM sucrose (Fisher Scientific), pH 7.15), to remove the CNS (ventral nerve cord and brain lobes). The isolated CNS was then transferred to a droplet of external saline, within which it was laid flat (dorsal side up) and glued (GLUture Topical Tissue Adhesive; World Precision Instruments USA) to a Sylgard-coated cover slip (1 to 2mm depth of cured SYLGARD Elastomer (Dow-Corning USA) on a 22 x 22mm square coverslip). The preparation was then placed on a glass slide and viewed under a microscope (Olympus BX51-WI).

Calcium imaging

Dissected CNSs were imaged (QImaging EXi-Aqua; photometrics, Arizona, US) with an acquisition frame rate of 10Hz and frame duration of 100 ms using a x20 immersion lens. GCaMP8f was excited using a 470 nm collimated LED (Thorlabs, New Jersey, US). Time-course of neuronal fluorescence was determined in WinFluor (V.4.1.5; University of Strathclyde, UK) by adding regions of interest (ROIs) to axons, close to the cell body (Streit et al, 2016). In Clampfit (10.3.1.5; Molecular Devices, California, US) fluorescence traces were smoothed using a lowpass BoxCar filter using 11 smoothing points prior to analysis.

For motoneuron calcium transients (Fig.1), recordings were conducted for 600s, whilst temperature of the explanted CNS was increased steadily from ~23°C to ~34°C using a digital heating unit (CO 102; Linkam Scientific, Surrey, UK). For sham recordings, temperature was maintained at a constant 25°C. Temperature was measured in Clampex (10.3.1.5; Molecular Devices, California, US) using a temperature sensor placed in the external saline surrounding the brain, via a temperature controller (TC-10; npi electronic GmbH, Tamm, Germany). The frequency of calcium fluorescence peaks was measured for each segment (A8/9 – A1) in three sequential 200 s time periods and averaged per larva. Average temperature was calculated for each recording during these same 200 s time periods.

For calcium imaging of interneurons after CP manipulation (Fig.5), 180 s recordings were taken. Time lag was determined by manually assessing the time between peak fluorescence corresponding to ipsilaterally adjacent interneurons (segments A6 – A1. For each recording the first complete forward waves of activity were used (up to three repeats per trace) to generate an average intersegment duration for each pair of interneurons.

Whole cell patch clamp electrophysiology

CNSs were dissected, mounted (see calcium imaging methods) and viewed under a 60x water-immersion lens. To access soma, 1% protease (Streptomyces griseus, Type XIV, Sigma-Aldrich, in external saline) contained within a wide-bore glass pipette (GC100TF-10; Harvard Apparatus UK, approx. 10 µm opening) was applied to abdominal segments, roughly between A5-A2 (Baines and Bate, 1998). This was done to remove overlaying glia to facilitate access to underlying nerve cell soma (e.g., aCC). Motoneurons were identified by anatomical position and relative cell size, with aCC being positioned close to the midline and containing both an ipsilateral and contralateral projection. Recordings were made using borosilicate glass pipettes (GC100F-10, Harvard Apparatus) that were fire polished to resistances of 10 - 15MΩ when filled with intracellular saline (140 mM potassium-D-gluconate (Sigma-Aldrich), 2 mM $MgCl_2 \cdot 6H_2O$ (Sigma-Aldrich), 2 mM EGTA (Sigma-Aldrich), 5 mM KCl (Fisher Scientific), and 20 mM HEPES (Sigma-Aldrich), (pH 7.4). Input resistance was measured in the 'whole cell' configuration, and only cells that had an input resistance ≥ 0.5 GΩ were used for experiments. Cell capacitance and break-in resting membrane potential was also measured for each cell recorded. Data for current steps recordings was captured using a Multiclamp 700B amplifier controlled by pCLAMP (version 10.7.0.3), via an analogue-to-digital converter (Digidata 1440A, Molecular Devices). Whole cell recordings measuring synaptic drive to motoneurons and spontaneous motoneurons activity were conducted using an amplifier (Axopatch 1D) controlled by pCLAMP (V.10.3.1.5) by an analog-to- digital converter (Digidata 1322A, Molecular Devices. Trace/s were sampled at 20 kHz and filtered online at 10 kHz.

Current step recordings

Mecamylamine (200 μM in saline) was used to block postsynaptic nACh receptors in order to synaptically isolate neurons for experiments designed to measure intrinsic motoneuron excitability. Once patched, neurons were brought to a membrane potential of -60 mV using current injection. Each recording consisted of 20 x 4 pA (500 ms) current steps, including an initial negative step, giving a range of -4 to +72 pA. Number of spikes were counted and plotted against injected current. Both cell capacitance and input resistance were compared between conditions to ensure that any observed differences in excitability were not due to differences in either cell size or resistance.

Synaptic drive to motoneurons

To measure synaptic drive between A27h pre-motor interneurons and aCC, A27h neurons were identified via *Chronos-mVenus* reporter (as above), allowing corresponding aCC motoneurons to be patched. Recordings were conducted in current-clamp, with current injected into aCC sufficient to evoke a mean spike frequency of ~10-20 Hz, prior to optogenetic stimulation. Recordings consisted of: individual sweeps, beginning with 1 s LED off, followed by 1 s LED on, and 1 s LED off (repeated 5-8 times per cell). Change in AP frequency (%) was calculated for each recording (per sweep) comparing AP frequency before and during stimulation, which was then averaged for each cell.

Spontaneous rhythmic currents (SRCs) were recorded for 180 s with aCC voltage clamped at -60 mV. Amplitude, duration, and frequency were measured for the first 15 events of each trace using Clampfit's event detection, threshold search, function. The first 15 events with a stable baseline, an amplitude of >300 pA and no double peaks were accepted for analysis. Amplitude was measured as the change from baseline immediately prior to event initiation to the peak current and normalised for cell capacitance, providing a measure of current density. SRC duration was measured as the width of an event at 100 pA amplitude.

Spontaneous motoneuron recordings

Motoneuron spontaneous activity was recorded using an adapted whole cell current clamp protocol, in I=0, to measure passive action potential bursting properties. In Clampfit (version 10.3.1.5), 180 s recordings, were analysed to detect action potential 'spike times'. These were imported into MATLAB and analysed using a custom script (developed by Mituzaite et al., 2021). An action potential burst was considered as an

event consisting of at least 3 spikes occurring within 100 ms and ending when no spike was detected for 100 ms.

Crawling Assay

Crawling behaviour was recorded at the mid-third instar stage, 72 hours after larval hatching (ALH). Larvae were rinsed in water and placed inside a 24cm x 24cm crawling arena with a base of 5mm thick 0.8% agarose gel (Bacto Agar), situated inside an incubator. Temperature was maintained at 25±0.5°C, reported via a temperature probe in the agar medium. Humidity was kept constant. Larval crawling was recorded using a frustrated total internal reflection-based imaging method (FIM) in conjunction with the tracking software FIMTrack (Risse et al., 2013, 2017) using a Basler acA2040-180km CMOS camera, fitted with a 16mm KOWA-IJM3sHC.SW-VIS-NIR lens, acquisition controlled by Pylon software (Basler) and Streampix (v.6) software (NorPix). Larvae were recorded for 20 minutes at five frames per second.

Recordings were split into four 5-minute sections with the first five minutes of acclimatisation discarded. The remaining three 5-minute sections were used to analyse crawling speed, choosing crawling periods of uninterrupted forward crawling, devoid of pauses, turning or collision events. Each larva was sampled up to once per 5-minute section. Crawling speed was calculated using FIMTrack software.

Statistics

Statistical analyses were done using GraphPad Prism Software (Version 10.1.2). Datasets were tested for normal distribution with the Shapiro-Wilk Test. Normally distributed data were then tested with students t-test (for pairwise comparison). Normally distributed analysis for more than two groups was done with a one-way ANOVA and post hoc tested with a Tukey multiple comparison test. Non-normally distributed data sets of two groups were tested with Mann-Whitney U Test (pairwise comparison) and datasets with more than two groups were tested with a Kruskal Wallis ANOVA and post hoc tested with a Dunns multiple post hoc comparison test. For whole cell electrophysiology experiments in isolated neurons, linear regression analysis was used to compare the intercepts between conditions. This analysis was restricted to linear sections of data, represented by inset graphs. For all datasets mean and standard error of mean (SEM) are shown. Significance levels were * $p<0.05$; ** $p<0.01$; *** $p<0.001$; **** $p<0.0001$

References

Ashburner, M., Carson, H. L., & Thompson, J. N. (1983). Ectophysilogy: Abiotic Factors. In *The Genetics and Biology of Drosophila,* (3rd ed., pp. 105–170).

Baines, R. A., Robinson, S. G., Fujioka, M., Jaynes, J. B., & Bate, M. (1999). Postsynaptic expression of tetanus toxin light chain blocks synaptogenesis in Drosophila. *Current Biology*, *9*(21), 1267-S1. https://doi.org/10.1016/S0960-9822(99)80510-7

Baines, R. A., Uhler, J. P., Thompson, A., Sweeney, S. T., & Bate, M. (2001). Altered Electrical Properties in Drosophila Neurons Developing without Synaptic Transmission. *The Journal of Neuroscience*, *21*(5), 1523–1531. https://doi.org/10.1523/JNEUROSCI.21-05-01523.2001

Carreira-Rosario, A., York, R. A., Choi, M., Doe, C. Q., & Clandinin, T. R. (2021). Mechanosensory input during circuit formation shapes Drosophila motor behavior through patterned spontaneous network activity. *Current Biology*, *31*(23), 5341-5349.e4. https://doi.org/10.1016/j.cub.2021.08.022

Coulson, B., Hunter, I., Doran, S., Parkin, J., Landgraf, M., & Baines, R. A. (2022). Critical periods in Drosophila neural network development: Importance to network tuning and therapeutic potential. *Frontiers in Physiology*, *13*(December), 1–11. https://doi.org/10.3389/fphys.2022.1073307

Crisp, S., Evers, J. F., Fiala, A., & Bate, M. (2008). The development of motor coordination in Drosophila embryos. *Development*, *135*(22), 3707–3717. https://doi.org/10.1242/dev.026773

Crisp, S. J., Evers, J. F., & Bate, M. (2011). Endogenous Patterns of Activity Are Required for the Maturation of a Motor Network. *Journal of Neuroscience*, *31*(29), 10445–10450. https://doi.org/10.1523/JNEUROSCI.0346-11.2011

Delvendahl, I., & Müller, M. (2019). Homeostatic plasticity—a presynaptic perspective. *Current Opinion in Neurobiology*, *54*, 155–162. https://doi.org/10.1016/j.conb.2018.10.003

Dombrovski, M., & Condron, B. (2021). Critical periods shaping the social brain: A perspective from Drosophila. *BioEssays*, *43*(1), 2000246. https://doi.org/10.1002/bies.202000246

Dyson, A., Ryan, M., Garg, S., Evans, D. G., & Baines, R. A. (2022). Loss of NF1 in Drosophila Larvae Causes Tactile Hypersensitivity and Impaired Synaptic Transmission at the Neuromuscular Junction. *Journal of Neuroscience*, *42*(50), 9450–9472. https://doi.org/10.1523/JNEUROSCI.0562-22.2022

Feng, Y., Ueda, A., & Wu, C. F. (2004). A modified minimal hemolymph-like solution, HL3.1, for physiological recordings at the neuromuscular junctions of normal and mutant Drosophila larvae. *Journal of Neurogenetics*, *18*(2), 377–402. https://doi.org/10.1080/01677060490894522

Frank, C. A., James, T. D., & Müller, M. (2020). Homeostatic control of Drosophila neuromuscular junction function. *Synapse*, *74*(1), 22133. https://doi.org/10.1002/syn.22133

Frank, C. A., Kennedy, M. J., Goold, C. P., Marek, K. W., & Davis, G. W. (2006). Mechanisms Underlying the Rapid Induction and Sustained Expression of Synaptic Homeostasis. *Neuron*, *52*(4), 663–677. https://doi.org/10.1016/j.neuron.2006.09.029

Fujioka, M., Lear, B. C., Landgraf, M., Yusibova, G. L., Zhou, J., Riley, K. M., Patel, N. H., & Jaynes, J. B. (2003). Even-skipped, acting as a repressor, regulates axonal projections in Drosophila. *Development*, *130*(22), 5385–5400. https://doi.org/10.1242/dev.00770

Fushiki, A., Kohsaka, H., & Nose, A. (2013). Role of Sensory Experience in Functional Development of Drosophila Motor Circuits. *PLoS ONE*, *8*(4), e62199. https://doi.org/10.1371/journal.pone.0062199

Genç, Ö., & Davis, G. W. (2019). Target-wide Induction and Synapse Type-Specific Robustness of Presynaptic Homeostasis. *Current Biology*, *29*(22), 3863-3873.e2. https://doi.org/10.1016/j.cub.2019.09.036

Giachello, C. N. G., & Baines, R. A. (2015). Inappropriate Neural Activity during a Sensitive Period in Embryogenesis Results in Persistent Seizure-like Behavior. *Current Biology*, *25*(22), 2964–2968. https://doi.org/10.1016/j.cub.2015.09.040

Giachello, C. N. G., Fan, Y. N., Landgraf, M., & Baines, R. A. (2019). Activity manipulation of an

excitatory interneuron, during an embryonic critical period, alters network tuning of the Drosophila larval locomotor circuit. In *bioRxiv* (p. 780221). bioRxiv. https://doi.org/10.1101/780221

Giachello, C. N. G., Fan, Y. N., Landgraf, M., & Baines, R. A. (2021). Nitric oxide mediates activity-dependent change to synaptic excitation during a critical period in Drosophila. *Scientific Reports*, *11*(1), 1–12. https://doi.org/10.1038/s41598-021-99868-8

Giachello, C. N. G., Zarin, A. A., Kohsaka, H., Fan, Y. N., Nose, A., Landgraf, M., & Baines, R. A. (2020). Electrophysiological validation of premotor interneurons monosynaptically connected to the aCC motoneuron in the Drosophila larval CNS. *BioRxiv*, 1–19. https://doi.org/10.1101/2020.06.17.156430

Goel, P., & Dickman, D. (2021). Synaptic homeostats: latent plasticity revealed at the Drosophila neuromuscular junction. In *Cellular and Molecular Life Sciences* (Vol. 78, Issue 7, pp. 3159–3179). Springer Science and Business Media Deutschland GmbH. https://doi.org/10.1007/s00018-020-03732-3

Hageter, J., Starkey, J., Horstick, E. J., Hageter, J., Starkey, J., & Horstick, E. J. (2023). Article Thalamic regulation of a visual critical period and motor behavior ll ll Thalamic regulation of a visual critical period and motor behavior. *CellReports*, *42*(4), 112287. https://doi.org/10.1016/j.celrep.2023.112287

Harrison, R. V, Gordon, K. A., & Mount, R. J. (2005). Is There a Critical Period for Cochlear Implantation in Congenitally Deaf Children ? Analyses of Hearing and Speech Perception Performance after Implantation. *Developmental Psychobiology*, *46*(3), 155–292. https://doi.org/DOI 10.1002/dev.20052

Hensch, T. K. (2004). Critical period regulation. In *Annual Review of Neuroscience* (Vol. 27, pp. 549–579). https://doi.org/10.1146/annurev.neuro.27.070203.144327

Hensch, T. K. (2005). Critical period plasticity in local cortical circuits. In *Nature Reviews Neuroscience* (Vol. 6, Issue 11, pp. 877–888). Nature Publishing Group. https://doi.org/10.1038/nrn1787

Hensch, T. K., & Quinlan, E. M. (2018). Critical periods in amblyopia. In *Visual neuroscience* (Vol. 35, p. E014). Cambridge University Press. https://doi.org/10.1017/S0952523817000219

Hess, E. H. (1975). Imprinting: Early experience and the dvelopmental psychobiology of attachment. *Psychosomatic Medicine*, *37*(2), 188–190.

Horn, G. (2004). Pathways of the past: the imprint of memory. *Nature Reviews Neuroscience*, *5*(February), 108–121. https://doi.org/10.1038/nrn1324

Hubel, D. H., & Wiesel, T. N. (1970). The period of susceptibility to the physiological effect of unilateral eye closure in kittens. *Journal of Physiology*, *206*, 419–436. https://doi.org/10.1113/jphysiol.1970.sp009022

Hunter, I., Coulson, B., Pettini, T., Davies, J. J., Parkin, J., Landgraf, M., & Baines, R. A. (2024). Balance of activity during a critical period tunes a developing network. *ELife*, *12*, 1–23. https://doi.org/10.7554/eLife.91599

Hunter, I., Coulson, B., Zarin, A. A., & Baines, R. A. (2021). The Drosophila Larval Locomotor Circuit Provides a Model to Understand Neural Circuit Development and Function. In *Frontiers in Neural Circuits* (Vol. 15, p. 62). Frontiers Media S.A. https://doi.org/10.3389/fncir.2021.684969

Johnson, B. R., Hauptman, S. A., & Bonow, R. H. (2007). Construction of a Simple Suction Electrode for Extracellular Recording and Stimulation. *Journal of Undergraduate Neuroscience Education*, *6*(1), A21.

Jusyte, M., Blaum, N., Böhme, M. A., Berns, M. M. M., Bonard, A. E., Vámosi, Á. B., Pushpalatha, K. V., Kobbersmed, J. R. L., & Walter, A. M. (2023). Unc13A dynamically stabilizes vesicle priming at synaptic release sites for short-term facilitation and homeostatic potentiation. *Cell Reports*, *42*(6). https://doi.org/10.1016/j.celrep.2023.112541

Kiral, F. R., Dutta, S. B., Linneweber, G. A., Hilgert, S., Poppa, C., Duch, C., von Kleist, M., Hassan, B. A., & Hiesinger, P. R. (2021). Brain connectivity inversely scales with developmental temperature in Drosophila. *Cell Reports*, *37*(12), 110145. https://doi.org/10.1016/j.celrep.2021.110145

Kratschmer, P., Lowe, S. A., Buhl, E., Chen, K., Kullmann, D. M., Pittman, A., Hodge, J. J. L., & Jepson, J. E. C. (2021). Impaired Pre-Motor Circuit Activity and Movement in a Drosophila Model of KCNMA1 -Linked Dyskinesia. *Movement Disorders*, *36*(5), 1158–1169. https://doi.org/10.1002/mds.28479

Landgraf, M., Jeffrey, V., Fujioka, M., Jaynes, J. B., & Bate, M. (2003). Embryonic Origins of a Motor System: Motor Dendrites Form a Myotopic Map in Drosophila. *PLoS Biology*, *1*(2), e41. https://doi.org/10.1371/journal.pbio.0000041

Lee, Y., & Montell, C. (2013). Drosophila TRPA1 functions in temperature control of circadian rhythm in pacemaker neurons. *Journal of Neuroscience*, *33*(16), 6716–6725. https://doi.org/10.1523/JNEUROSCI.4237-12.2013

Lowe, S. A., Wilson, A. D., Aughey, G. N., Banjaree, A., Goble, T., Simon-Batsford, N., Sanderson, A., Kratschmer, P., Balogun, M., Gao, H., Aw, S. S., & Jepson, J. E. C. (2023). BK channel gain-of-function disrupts limp control by suppressing neurotransmission during a critical developmental window. *BioRxiv*. https://doi.org/10.1101/2023.09.20.558625

Marder, E. (2023). Individual Variability, Statistics, and the Resilience of Nervous Systems of Crabs and Humans to Temperature and Other Perturbations. *Eneuro*, *10*(11), ENEURO.0425-23.2023. https://doi.org/10.1523/ENEURO.0425-23.2023

Marder, E., & Rue, M. C. P. (2021). From the Neuroscience of Individual Variability to Climate Change. *The Journal of Neuroscience*, *41*(50), 10213–10221. https://doi.org/10.1523/JNEUROSCI.1261-21.2021

Müller, M., & Davis, G. W. (2012). Transsynaptic control of presynaptic Ca 2+ influx achieves homeostatic potentiation of neurotransmitter release. *Current Biology*, *22*(12), 1102–1108. https://doi.org/10.1016/j.cub.2012.04.018

Nardou, R., Sawyer, E., Song, Y. J., Wilkinson, M., Padovan-Hernandez, Y., de Deus, J. L., Wright, N., Lama, C., Faltin, S., Goff, L. A., Stein-O'Brien, G. L., & Dölen, G. (2023). Psychedelics reopen the social reward learning critical period. *Nature*, *618*(7966), 790–798. https://doi.org/10.1038/s41586-023-06204-3

Oswald, M. C. W., Brooks, P. S., Zwart, M. F., Mukherjee, A., West, R. J. H., Giachello, C. N. G., Morarach, K., Baines, R. A., Sweeney, S. T., & Landgraf, M. (2018). Reactive oxygen species regulate activity-dependent neuronal plasticity in Drosophila. *ELife*, *7*. https://doi.org/10.7554/eLife.39393

Peled, E. S., & Isacoff, E. Y. (2011). Optical quantal analysis of synaptic transmission in wild-type and rab3-mutant Drosophila motor axons. *Nature Neuroscience*, *14*(4), 519–526. https://doi.org/10.1038/nn.2767

Pérez-Moreno, J. J., & O'Kane, C. J. (2019). GAL4 Drivers Specific for Type Ib and Type Is Motor Neurons in Drosophila. *G3 Genes|Genomes|Genetics*, *9*(2), 453–462. https://doi.org/10.1534/g3.118.200809

Powsner, L. (1935). The Effects of Temperature on the Durations of the Developmental Stages of Drosophila melanogaster. *Physiological Zoology*, *8*(4), 474–520. https://doi.org/10.1086/physzool.8.4.30151263

Risse, B., Berh, D., Otto, N., Klämbt, C., & Jiang, X. (2017). FIMTrack: An open source tracking and locomotion analysis software for small animals. *PLoS Computational Biology*, *13*(5), 1–15. https://doi.org/10.1371/journal.pcbi.1005530

Risse, B., Thomas, S., Otto, N., Löpmeier, T., Valkov, D., Jiang, X., & Klämbt, C. (2013). FIM, a Novel FTIR-Based Imaging Method for High Throughput Locomotion Analysis. *PLoS ONE*, *8*(1), 1–11. https://doi.org/10.1371/journal.pone.0053963

Scialò, F., Sriram, A., Naudí, A., Ayala, V., Jové, M., Pamplona, R., & Sanz, A. (2015). Target of rapamycin activation predicts lifespan in fruit flies. *Cell Cycle*, *14*(18), 2949–2958. https://doi.org/10.1080/15384101.2015.1071745

Sigrist, S. J., Reiff, D. F., Thiel, P. R., Steinert, J. R., & Schuster, C. M. (2003). Experience-Dependent Strengthening of Drosophila Neuromuscular Junctions. *The Journal of Neuroscience*, *23*(16),

6546–6556. https://doi.org/10.1523/JNEUROSCI.23-16-06546.2003

Soiza-Reilly, M., & Azcurra, J. M. (2009). Developmental striatal critical period of activity-dependent plasticity is also a window of susceptibility for haloperidol induced adult motor alterations. *Neurotoxicology and Teratology*, *31*(4), 191–197. https://doi.org/10.1016/j.ntt.2009.03.001

Sulkowski, M. J., Han, T. H., Ott, C., Wang, Q., Verheyen, E. M., Lippincott-Schwartz, J., & Serpe, M. (2016). A Novel, Noncanonical BMP Pathway Modulates Synapse Maturation at the Drosophila Neuromuscular Junction. *PLoS Genetics*, *12*(1), e1005810. https://doi.org/10.1371/journal.pgen.1005810

Valdes-Aleman, J., Fetter, R. D., Sales, E. C., Heckman, E. L., Venkatasubramanian, L., Doe, C. Q., Landgraf, M., Cardona, A., & Zlatic, M. (2021). Comparative Connectomics Reveals How Partner Identity, Location, and Activity Specify Synaptic Connectivity in Drosophila. *Neuron*, *109*(1), 105-122.e7. https://doi.org/10.1016/j.neuron.2020.10.004

Williamson, M., Mitchell, A., & Condron, B. (2021). Birth temperature followed by a visual critical period determines cooperative group membership. *Journal of Comparative Physiology A: Neuroethology, Sensory, Neural, and Behavioral Physiology*, *207*(6), 739–746. https://doi.org/10.1007/s00359-021-01512-3

Winding, M., Pedigo, B. D., Barnes, C. L., Patsolic, H. G., Park, Y., Kazimiers, T., Fushiki, A., Andrade, I. V, Khandelwal, A., Valdes-aleman, J., Li, F., Randel, N., Barsotti, E., Correia, A., Fetter, R. D., Hartenstein, V., Priebe, C. E., Vogelstein, J. T., Cardona, A., & Zlatic, M. (2023). The connectome of an insect brain. *Science*, *379*(aeadd9330). https://doi.org/10.1126/science.add9330

Zeng, X., Komanome, Y., Kawasaki, T., Inada, K., Jonaitis, J., Pulver, S. R., Kazama, H., & Nose, A. (2021). An electrically coupled pioneer circuit enables motor development via proprioceptive feedback in Drosophila embryos. *Current Biology*, *31*(23), 5327-5340.e5. https://doi.org/10.1016/j.cub.2021.10.005

Zhong, Y., & Wu, C.-F. (2004). Neuronal Activity and Adenylyl Cyclase in Environment-Dependent Plasticity of Axonal Outgrowth in Drosophila. *The Journal of Neuroscience*, *24*(6), 1439–1445. https://doi.org/10.1523/JNEUROSCI.0740-02.2004

Züfle, P., Batista, L. L., Brandão, S. C., D'Uva, G., Christian, D., & Martelli, C. (2023). Metabolic constraints on growth explain how developmental temperature scales synaptic connectivity relevant for behaviour. *BioRxiv*, 2023.10.15.562389. https://www.biorxiv.org/content/10.1101/2023.10.15.562389v1%0Ahttps://www.biorxiv.org/content/10.1101/2023.10.15.562389v1.abstract